$\boldsymbol{A}_{rel}$ – Investigating $[Eu(H_2O)_9]^{3+}$ photophysics and creating a method to by-pass luminescence quantum yield determinations

*Nicolaj Kofod, Patrick Nawrocki, and Thomas Just Sørensen**

Department of Chemistry & Nano-Science Center, University of Copenhagen,

Universitetsparken 5, 2100 København Ø

Corresponding Author

tjs@chem.ku.dk

ABSTRACT

Lanthanide luminescence has been treated separate from molecular photophysics, although the underlying phenomena are the same. As the optical transitions observed in the trivalent lanthanide ions are forbidden, they do belong to the group that molecular photophysics have yet to conquer, yet the experimental descriptors remains valid. Determining these have proven challenging as full control/knowledge of sample composition is a prerequisite. This has been achieved, and here the luminescence quantum yields (ϕ_{lum}), luminescence lifetimes (τ_{obs}), oscillator strengths (f), and the rates of non-radiative (k_{nr}) and radiative ($k_r \equiv \boldsymbol{A}$) deactivation of $[Eu(H_2O)_9]^{3+}$ was determined for the trigonal tricapped prismatic (TTP) coordination geometry. Further, it was shown that instead

of a full photophysical characterization, it is possible to relate changes in transition probabilities to the relative parameter $\boldsymbol{A}_{\mathrm{rel}}$, which does not require reference data. While $\boldsymbol{A}_{\mathrm{rel}}$ does not afford comparisons between experiments, it resolves emission intensity changes due to emitter properties—changes in $\boldsymbol{A}$—from intensity changes due to environmental effects—changes in k_{nr}, and differences in the number of photons absorbed. When working with fluorescence this may seem trivial, when working with lanthanide luminescence it is not.

TOC GRAPHICS

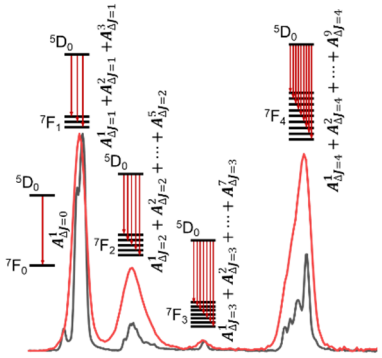

KEYWORDS Lanthanide luminescence, molecular photophysics, Europium(III) photophysics, quantum yields, $\boldsymbol{A}_{\mathrm{rel}}$

Introduction. Lanthanide luminescence is used in highly sensitive time-resolved and dissociation enhanced DELFIA bioassays,[1-3] in display and lighting technology,[4] and in lasers and telecommunication[5-6]. All application relies on the robust, atom-like, narrow and highly defined absorption and emission lines of the trivalent lanthanide ions. The optical transitions between the states in a trivalent lanthanide ion are all *forbidden* due to symmetry, spin, overlap, and momentum conservation. Molecular photophysics rationalize *allowed* optical transitions in molecules, and has strong experimental descriptors.[7-8] As molecular photophysics dictates that an observable can be related to specific molecular structure, the union of lanthanide luminescence and molecular

photophysics has been challenged by both the *forbidden* nature of the transitions and the complexity of solutions containing lanthanide(III) ions.[9-10] We will claim that the latter is a solved issue, and here we apply molecular photophysics to the study of europium(III) aqua ions in mixtures of H_2O and D_2O.[11-13]

Europium(III) ions, with strong luminescence in the red, is one of the most studied lanthanides. There are more than 9,000 papers on europium luminescence on Web of Science, a number that has been growing exponentially for more than a decade.[14] The appeal of europium(III) luminescence lies in that it is highly sensitive to various environmental effects,[15-17] and can thus be used in optical sensors, to document self-assembly,[18-19] and for bioimaging[2, 20-22]. More recently, europium(III) luminescence has evolved to be a highly effective tool for determining the structure, speciation and electronic structure of europium(III) complexes in solution.[9, 13, 23-28] This is possible as the transition probability of the electronic transitions in lanthanide(III) ions are directly correlated to—and change with—the ligand field symmetry, and thus inform on speciation and structure of the lanthanides(III) ions in solution. To obtain this information it is crucial to use transition probabilities and not emission intensities, as the latter depends on much more than molecular structure. Emission intensities are contingent on the number of photons absorbed as well as quenching by the environment, in particular via excited state energy transfer to vibrational overtones and high-energy phonons.[24, 29]

Europium(III) ions are well-suited to be treated using molecular photophysics as it—unique among the luminescent lanthanides—has a non-degenerate electronic ground state ($^7F_0$) and a non-degenerate emitting state ($^5D_0$). More than one state has to be considered for the other lanthanides, which makes it hard to assign individual lines in the spectra to single transitions. But for europium(III) we do not have this problem, and with a fixed speciation, we can investigate the

photophysics of distinct europium(III) species and address the issues with using emission intensity to quantify changes in europium(III) speciation. To do so we take a deep dive in molecular photophysics starting from Einstein's description of radiative transitions, considering the number of lines in each europium(III) emission band, and finishing by comparing our considerations to seven data points. The data is from seven samples with identical speciation, but different photophysics, prepared by dissolving europium(III) triflate in H_2O/ D_2O mixtures. The data allows us to map the fundamental photophysical properties of the europium(III) aqua ion. Further, we suggest that if europium(III) luminescence is to be used as an analytical tool, a new parameter $\boldsymbol{A}_{\mathrm{rel}}$ should be used instead of emission intensity.

Experimental section.

Sample preparation. All chemicals were used as received. 149-151 mg of $Eu(CF_3SO_3)_3$ (98% Strem Chemicals) was dissolved in mixtures of H_2O (from a milli-Q purification system) with 0.01 M $HClO_4$ (diluted from 65% $HClO_4$ from Prolabo) and D_2O (Eurisotop 99.90%D) with 0.01 M $DClO_4$ (diluted from 68% $DClO_4$ 99% atom D from Sigma-Aldrich). The europium(III) concentration was 0.050 M in all samples. Preliminary attempts to dry the $Eu(CF_3SO_3)_3$ revealed no changes in mass after 24 hours in an oven at 60 °C and 0.2 mbar. Samples were measured within 10 hours of preparation to avoid contamination with ambient water. Before measuring, samples were stored in closed glass vials further sealed with Parafilm M (Sigma-Aldrich). An unopened bottle of D_2O was used to further reduce contamination from ambient water. Coumarin-153 (C-153, $\Phi_f = 0.53 \pm 0.04$)[30] (99%, Sigma Aldrich) in ethanol (HPLC grade, Sigma Aldrich) was used as reference for quantum yield measurements. The stock solution of C-153 was made by dissolving a few grains of the dye in powder form in 5 mL ethanol. This stock solution was diluted until the absorbance was <0.1. All dilutions in the quantum yield determinations were made by

taking 3 mL of the previous sample and adding 1 mL of the solvent. The sample composition of the 7 samples used are shown in Table 1.

Table 1. Sample composition of measured Eu^{3+} samples. $x_{D/H}$ denotes the fractional volume of D_2O/H_2O. All samples contain 0.01 M of $XClO_4$ (X=D / H).

Sample #	$Eu(CF_3SO_3)_3$ (mg)	$[Eu(CF_3SO_3)_3]$ (M)	H_2O (mL)	D_2O (mL)	$x_{D/H}$
Eu1	151	0.050	5.00	0	0
Eu2	149	0.050	3.75	1.25	0.25
Eu3	150	0.050	2.50	2.50	0.5
Eu4	150	0.050	1.25	3.75	0.75
Eu5	149	0.050	0.75	4.25	0.85
Eu6	150	0.050	0.25	4.75	0.95
Eu7	151	0.050	0	1.00	1

Optical spectroscopy. Absorption spectra were measured on a Lambda800 double-beam spectrophotometer from PerkinElmer using a Horiba Xenon arc lamp as excitation source. The instrument was zeroed on an absolute scale using air as a reference (100% transmission) to a blocked beam (0% transmission). Slits were kept at 2 nm. Pure solvent was used as a reference during measurements. The reference solvent had the same H_2O/D_2O composition as the sample measured. Steady state emission spectra were measured on a PTI QuantaMaster8075 from Horiba Scientific using a halogen lamp as excitation source. The temperature was kept constant at 20°C using a Koolance EXT440 temperature control from Horiba Scientific. A constant flow of nitrogen gas was sent through the sample chamber to avoid condensation. Excitation was done at 394 nm. Emission and excitation slits were kept at 2 nm and 5 nm respectively. Wavelength dependence in the detector sensibility was corrected using a factory-provided correction file. Lamp fluctuations

was corrected using a reference detector. All absorption and steady state emission spectra were measured in 10 mm cuvettes from Starna Scientific.

Time-resolved emission spectra were measured on the same PTI QuantaMaster8075 instrument mentioned above using a Xenon Flash lamp as excitation source. Excitation was done at 394 nm and emission was measured at 700 nm. Slits were kept at 5 nm for both excitation and emission slits. A 300 μs time-gate was used to remove residual signal from the lamp. The decay traces were all fitted to mono-exponential decay functions using the OriginPro 2020 (OriginLab) software package. Temperature was kept constant at 20°C using the Koolance setup mentioned above. Time-resolved emission spectra were measured in a 2 mm path-length 0.8 mL quartz cuvette from Starna Scientific. Time-resolved spectroscopy were measured on the same samples as used in absorption and steady state emission at a later time (less than 5 hours) to avoid changing mirrors in the spectrometer. No other lanthanide signals were detected during measurements. All absorption spectra, emission spectra and decay traces can be found in the SI.

Quantum Yields. Quantum Yields were determined using the IUPAC recommended relative five-point dilution method using Coumarin-153 in ethanol as the reference dye ($\Phi_f = 0.53 \pm 0.04$).[30-32] The quantum yield is determined by eq. 1

$$\Phi_X = \Phi_r \cdot \frac{\int I_X^E}{Abs_X} \cdot \frac{Abs_r}{\int I_r^E} \cdot \frac{(\eta_X)^2}{(\eta_r)^2} \qquad \text{eq. 1}$$

Where Φ_X is the quantum yield of the sample, Φ_r is the quantum yield of the reference dye, $\int I^E_X$ and $\int I^E_r$ are the integrated emission intensity of the sample and the reference dye respectively, Abs_X and Abs_r are the absorbance at the wavelength of excitation of the sample and the reference dye respectively using the same slit widths as the excitations slits in the luminescence spectra, and η_X and η_r are the refractive index of the solvent of the sample and the reference dye respectively. The refractive index of H_2O (1.333) was used for all mixtures of H_2O and D_2O. From the quantum

yield and the excited state lifetime, we can determine the radiative and non-radiative rates of the excited state using eq. 2

$$\Phi = \frac{k_r}{k_r + k_{nr}} = k_r \cdot \tau_{obs} \quad \text{eq. 2}$$

Where Φ is the quantum yield, k_r is the radiative rate constant, k_{nr} is the non-radiative rate constant and τ_{obs} is the excited state lifetime. Absorbance was kept below 0.1 for all samples to avoid inner-filter effects.

Horrocks Equation. In order to determine the number of H_2O molecules in the inner coordination sphere we employ the Modified Horrocks Equation[24, 29, 33]

$$q = A\left(\left(\tau_{H_2O}\right)^{-1} - \left(\tau_{D_2O}\right)^{-1} - B\right) \quad \text{eq. 3}$$

Where A is 1.2 ms^{-1}, q is the number of inner sphere H_2O molecules, τ_{H2O} and τ_{D2O} are the observed excited state lifetimes in H_2O and D_2O respectively and B is the correction for outer sphere contributions which is 0.25 ms. In this study, we work with mixtures of D_2O and H_2O. To account for the changes in the fraction of protonated solvent molecules in the outer coordination sphere of B we instead use B′

$$B' = B \cdot x_{H/D} \quad \text{eq. 4}$$

Where B′ is the modified outer sphere correction, B is the outer sphere correction from the modified Horrocks equation, and $F_{H/D}$ is the mole fraction of H_2O in the sample. When employing eq. 3 we use the excited state lifetime of the pure D_2O sample (Eu7) for τ_{D2O} and the excited state lifetime of the sample as the τ_{H2O}.

Relative Transition probabilities. While emission intensity relates directly to the transition probability of emission, it is also affected by a number of external factors such as quenching, number of absorbed photons, concentration of emitter and instrumentation. This makes emission intensity a flawed measure compared to the radiative rate constant k_r obtained from quantum yields

or Einstein's coefficient of spontaneous emission $\boldsymbol{A}$. Both of these parameters are difficult to obtain, especially for lanthanide(III) ions. To circumvent this issue, we use the relative transition probability $\boldsymbol{A}_{\mathrm{rel}}$. For a series of emitters with similar concentrations, measured under similar conditions the relative quantum yield of emission can be defined as:

$$\Phi_{\mathrm{rel}} = \frac{\int I^{\mathrm{E}} d\lambda}{\mathrm{Abs}} \quad , \quad \Phi_{\mathrm{rel}}^{\lambda} = \frac{I^{\mathrm{E}}}{\mathrm{Abs}} \qquad \text{eq. 5}$$

Where Φ_{rel} is the relative quantum yield of emission, I^{E} emission intensity and Abs is the absorbance in the excitation window. This corrects the emission intensity for changes in the number of absorbed photons. As the quantum yield relates directly to the radiative rate constant k_r (eq. 2), which relates directly to Einstein's coefficient of spontaneous emission we can rewrite equation 6 as

$$\Phi_{\mathrm{rel}} = \frac{\boldsymbol{A}_{\mathrm{rel}}}{k_{\mathrm{obs}}} \quad , \quad \boldsymbol{A}_{\mathrm{rel}} = \Phi_{\mathrm{rel}} \cdot k_{\mathrm{obs}} = \frac{\Phi_{\mathrm{rel}}}{\tau_{\mathrm{obs}}} \quad , \quad \boldsymbol{A}_{\mathrm{rel}} = \frac{I^{\mathrm{E}}}{\mathrm{Abs} \cdot \tau_{\mathrm{obs}}} \qquad \text{eq. 6}$$

Where Φ_{rel} is the relative quantum yield of emission, $\boldsymbol{A}_{\mathrm{rel}}$ is the relative transition probability of emission, k_{obs} is the observed decay constant, τ_{obs} is the excited state lifetime, I^{E} is the emission intensity and Abs is the absorbance in the window of excitation.

Results and Discussion.

Einstein's constant for spontaneous emission. The probability of a radiative transition was described by Einstein as a rate constant of a unimolecular reactions[34-35]:

$$\boldsymbol{A} = k_{\mathrm{r}} = \frac{8\pi \cdot \eta^2 \cdot 2303}{N_{\mathrm{A}} \cdot c^2} \tilde{\nu}_{\mathrm{Em}}{}^3 \int \frac{\varepsilon(\nu_{\mathrm{A}})}{\nu_{\mathrm{A}}} d\nu_{\mathrm{A}} \qquad \text{eq. 7}$$

Where $\boldsymbol{A}$ is the transition probability, k_{r} is the radiative rate constant, η is the refractive index, N_{A} is Avogadro's number, c is the speed of light in vacuum, $\tilde{\nu}_{\mathrm{Em}}$ is the mean frequency of the emission band, ε is the molar absorption coefficient and ν_{A} is the frequency of absorption. Equation

7 describes the transition probability of spontaneous emission between two distinct electronic states.

The electronic energy levels of lanthanides as free ions in vacuum are often described by degenerate Russel-Saunders $^{S}L_{J}$ term symbols that arise from the electronic configuration when taking electron-electron repulsion and spin-orbit into account. When introduced into a chemical environment, the degeneracy is lifted by the ligand field, splitting and each $^{S}L_{J}$ energy level is resolved into one or more distinct electronic states.

Historically, the electronic transitions observed in *f*-elements were treated as $^{S}L_{J} \rightarrow {}^{S}L_{J}$ with a $2J+1$ degeneracy of the individual electronic energy level – a necessity as early instrumentation did not allow for resolving the underlying electronic states. As high-resolution spectra have become widely available, a more precise description can be obtained by considering the actual electronic states within the $^{S}L_{J}$ energy levels. This is a crucial step for better understanding the mechanisms and transition probabilities of *f-f* transitions as these are defined by the properties of the unique electronic states involved.

The relative intensities of the different bands in the europium(III)spectra has been described by the branching ratio—the differential emission probability between the $^{5}D_{0}$ state (the nondegenerate emissive energy level) and the groups of states within each of the $^{7}F_{J}$ levels—which is directly linked to the ligand field symmetry.[36-37] However, the number of states within the $^{7}F_{J}$ band is often ignored or used as a simple degeneracy. This treatment is problematic as there is no photophysical rationale for the transition probabilities of the states within the $^{S}L_{J}$ manifold to be equal. This is clear when high resolution is achieved as bands often split into peaks of varying intensity.[12, 38-39] When this level of detail is not achievable, care should be taken when rationalizing based on transition probabilities and branching ratios of bands instead of the actual transition lines. For all

lanthnide(III) ions bar europium(III) this becomes a significant challenge as each band contain numerous lines. Figure 1 shows the section of the europium(III) energy level manifold relevant for luminescence. It is readily seen that the number of states can be resolved when necessary, see Figure S42. Here, we are focus on the need to differentiate between observed emission intensity and actual transition probability. The latter is determined exclusively by electron structure, while the former is affected by several parameters.[40] Using the emission intensity as a single parameter in e.g. a binding study thus potentially leads to significant errors. The most accurate descriptor is the radiative rate of emission that is the transition probability $k_r \equiv \boldsymbol{A}$. This can be determined through from the emission quantum yield and luminescence lifetime, but obtaining accurate quantum yields is a laborious process even for ideal systems. It becomes particularly tricky for the weakly absorbing lanthanide(III) ions. In this work, we present a different pathway to obtaining an effective measure of the transition probability, a relative transition probability - $\boldsymbol{A}_{\mathrm{rel}}$. This parameter can be represented as a sum of transition probabilities of each band in the emission spectrum:

$$\boldsymbol{A}_{\mathrm{rel}} = \sum_{J=0}^{6} \boldsymbol{A}_{rel}^{\,{}^5D_0 \rightarrow {}^7F_J} \qquad \text{eq 8.}$$

As each $^5D_0 \rightarrow {}^7F_J$ band in equation 8 can be represented by a sum over the $2J+1$ transition lines it can be further expanded as done in equation 9:

$$\begin{aligned} \boldsymbol{A}_{\mathrm{rel}} = {} & \boldsymbol{A}_{rel}^{\,{}^5D_0 \rightarrow {}^7F_0} \\ & + \boldsymbol{A}_{rel}^{\,{}^5D_0 \rightarrow {}^7F_1^0} + \boldsymbol{A}_{rel}^{\,{}^5D_0 \rightarrow {}^7F_1^{+1}} + \boldsymbol{A}_{rel}^{\,{}^5D_0 \rightarrow {}^7F_1^{-1}} \\ & + \boldsymbol{A}_{rel}^{\,{}^5D_0 \rightarrow {}^7F_2^0} + \boldsymbol{A}_{rel}^{\,{}^5D_0 \rightarrow {}^7F_2^{+1}} + \boldsymbol{A}_{rel}^{\,{}^5D_0 \rightarrow {}^7F_2^{-1}} + \boldsymbol{A}_{rel}^{\,{}^5D_0 \rightarrow {}^7F_2^{+2}} + \boldsymbol{A}_{rel}^{\,{}^5D_0 \rightarrow {}^7F_2^{-2}} \\ & \ldots \end{aligned} \qquad \text{eq. 9}$$

For an europium(III) complex each line will have a unique and constant transition probability and it thus follows that the transition probability of each band and the overall transition probability determined from the spectrum must be constant. Any change in structure in the coordination sphere of an europium(III) ion will result in a change in the transition probability $\boldsymbol{A}$ which will be reported by $\boldsymbol{A}_{rel}$.[9, 13]

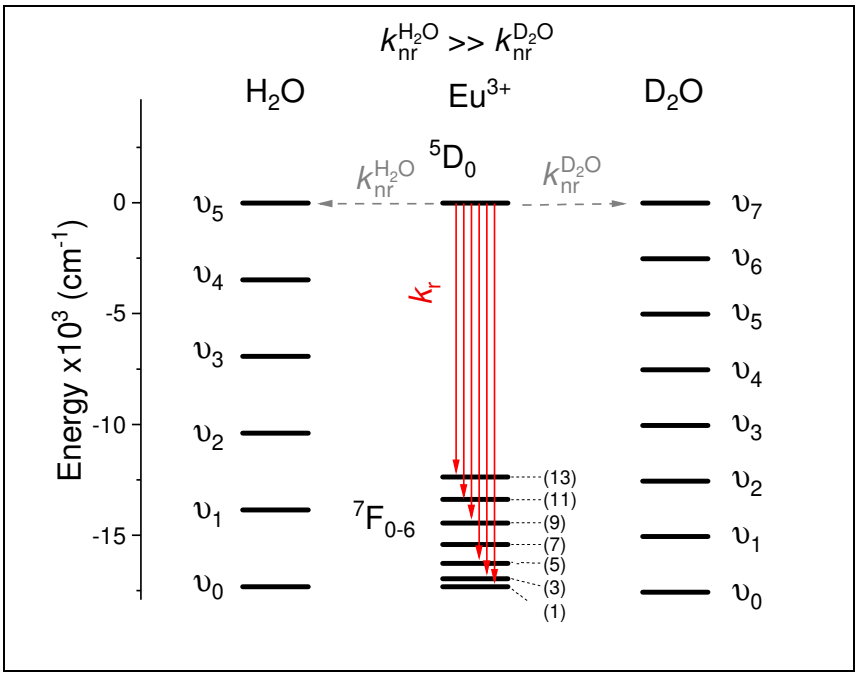

Figure 1. Illustration of the energy levels involved in the quenching of Eu^{3+} luminescence by H_2O and D_2O. The number in parenthesis denotes the number of states within the ^SL_J level

Speciation. Figure 2 (and Figures S1-S7) shows the absorption spectra of europium(III) in the seven water/heavy water mixtures (samples Eu1-Eu7). For each mixture five different concentrations of europium(III) is used. All spectra are identical and the absorbance is linear as a function of concentration. The identical spectra shows that the structure of the $[Eu(H_2O)_9]^{3+}$ ions are the same regardless of the mole fraction of heavy water ($x_{D/H}$). This is expected as the ligand

field is defined by the oxygen donor atoms and is unaffected by the isotope substitution of the protons. Note that the solutions has been slightly acidified (0.01 M H/$DClO_4$) in order to avoid the formation the monohydrixide $[Eu(H_2O)_8(OH)]^{2+}$. The linearity is evidence of a constant speciation and further ensures that no aggregates are formed as the concentration increase.

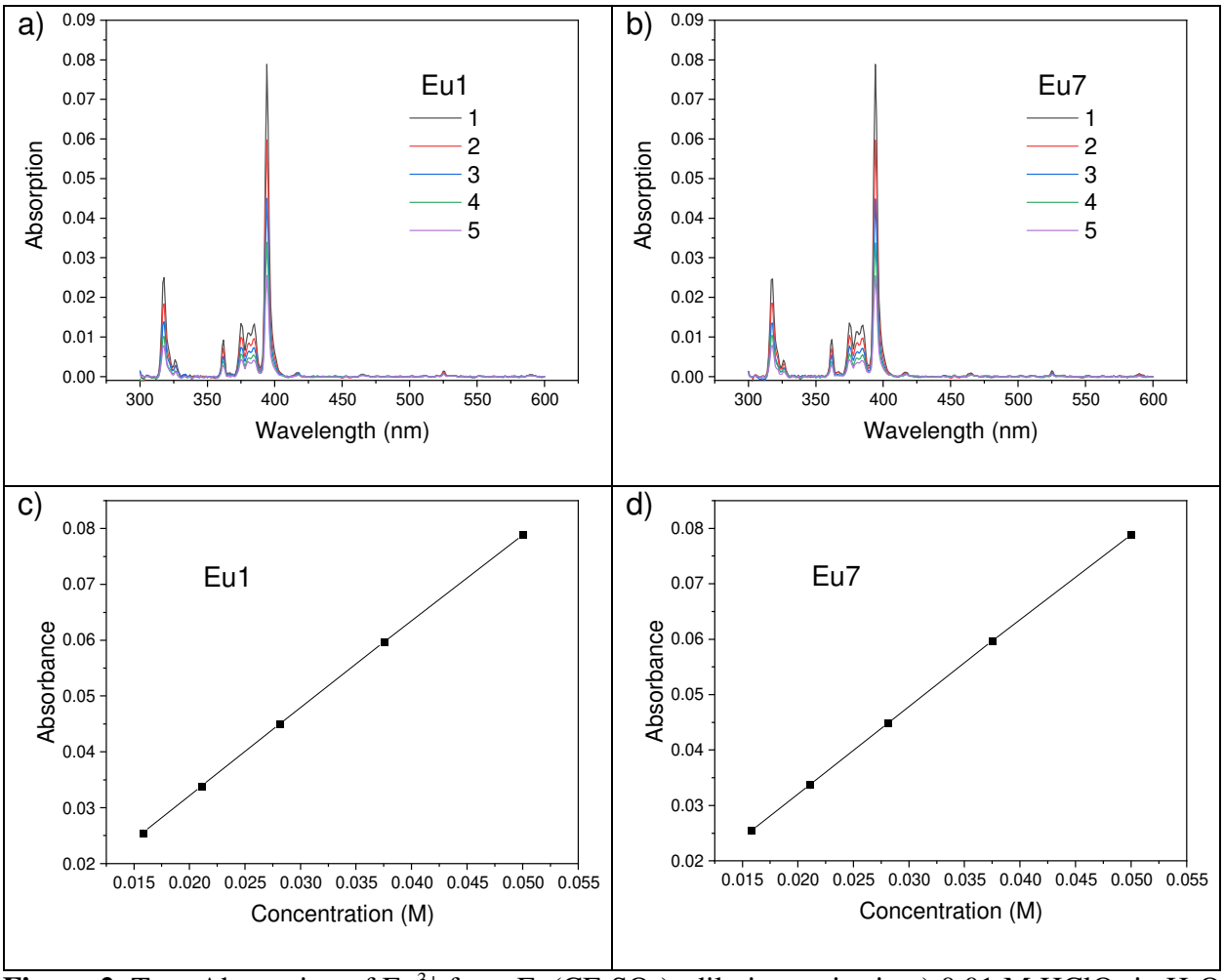

Figure 2. Top: Absorption of Eu^{3+} from $Eu(CF_3SO_3)_3$ dilution series in a) 0.01 M $HClO_4$ in H_2O ($x_{D/H}$ = 0) and b) 0.01 M $DClO_4$ in D_2O ($x_{D/H}$ = 1). Bottom: Absorbance at the excitation wavelength (394 nm) of Eu^{3+} from $Eu(CF_3SO_3)_3$ in a) 0.01 M $HClO_4$ in H_2O ($x_{D/H}$ = 0) and b) 0.01 M $DClO_4$ in D_2O ($x_{D/H}$ = 1) as a function of concentration. Line is a guide to the eyes only.

Figure 3 (and Figures S9-S15) shows the emission spectra of europium(III) in the seven water/heavy water mixtures (samples Eu1-Eu7) along with the integrated emission intensity as a

function of concentration. For each mixture five different concentrations of europium(III) is used. As in the absorption experiment, the shape of the spectra are all near identical, however with a 30-fold increase in intensity going from the pure water sample (Eu1) to the pure heavy water sample (Eu7). For the pure heavy water sample (Eu7), there is a slight increase in the relative ratio of the $^5D_0 \rightarrow {}^7F_4$ band compared to the $^5D_0 \rightarrow {}^7F_1$ band. We attribute this to an artefact arising from a slight defect in detector linearity. The $^5D_0 \rightarrow {}^7F_5$ and $^5D_0 \rightarrow {}^7F_6$ bands are only dectected in the higher $x_{D/H}$ samples (Eu6-Eu7, $x_{D/H} > 0.95$, Figures S14-S15). This is due to the low intensity of the bands and the poorer detector sensibility in the high wavelength region. It is not due to changes in structure. The peak visible at 560 nm is from the thermally populated $^5D_1 \rightarrow {}^7F_2$.[41] This peak is not included in the integrated emission intensity.

For samples with lower $x_{D/H}$ (Eu1-Eu4, Figures S9-S13) the emission intensities increase linearly with the concentration. In the higher $x_{D/H}$ samples (Eu5-Eu7, $x_{D/H} > 0.85$, Figure S13-S15) the intensity deviates from the linearity at higher concentrations. This is in accordance with a self-quenching effect found for europium(III) species in solution with long excited state lifetime at high concentrations in similar systems.[23]

As no spectral change is observed, we conclude that the structure and speciation across all 35 samples are constant.

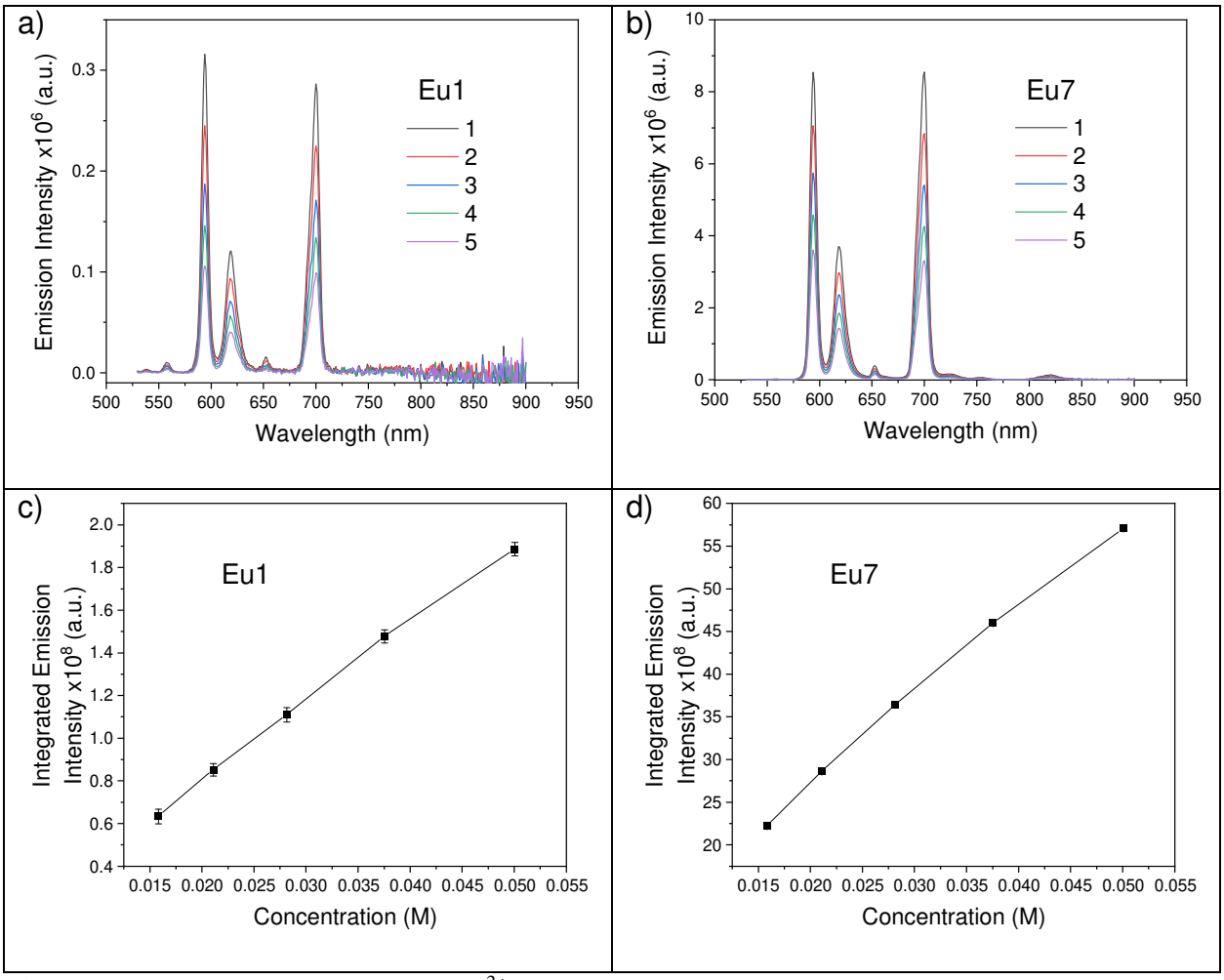

Figure 3. Top: Emission spectra of Eu^{3+} from $Eu(CF_3SO_3)_3$ dilution series in a) 0.01 M $HClO_4$ in H_2O ($x_{D/H}$ = 0) and b) 0.01 M $DClO_4$ in D_2O ($x_{D/H}$ = 1), excited at 394 nm. Bottom: Integrated emission intensity of Eu^{3+} from $Eu(CF_3SO_3)_3$ in a) 0.01 M $HClO_4$ in H_2O ($x_{D/H}$ = 0) and b) 0.01 M $DClO_4$ in D_2O ($x_{D/H}$ = 1) as a function of concentration. Line is a guide to the eyes only.

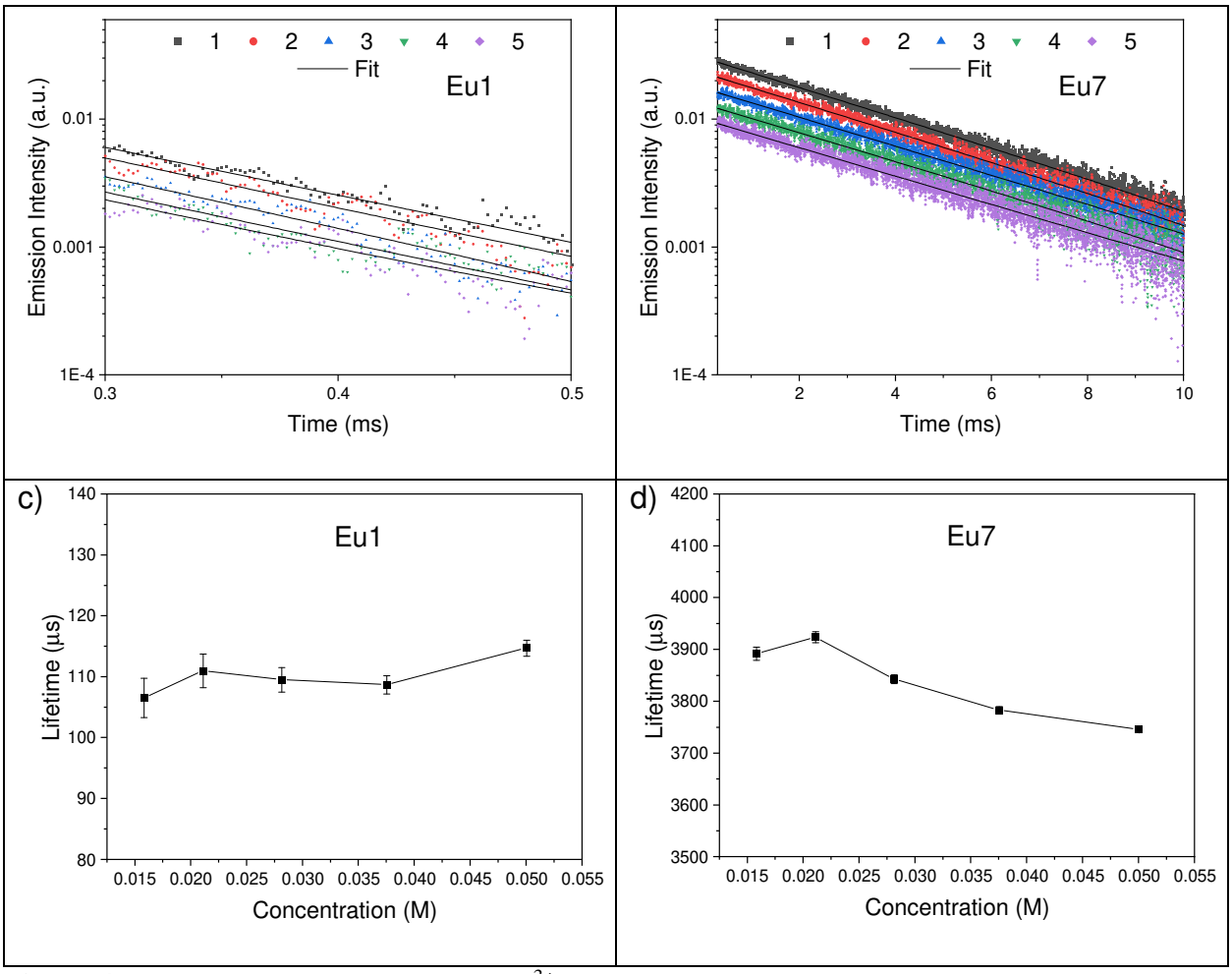

Figure 4. Top: Emission decay trace of Eu^{3+} from $Eu(CF_3SO_3)_3$ dilution series in a) 0.01 M $HClO_4$ in H_2O ($x_{D/H} = 0$) and b) 0.01 M $DClO_4$ in D_2O ($x_{D/H} = 1$), excited at 394 nm and measured at 700 nm. The data was fitted to a mono-exponential decay function. Bottom: Excited state lifetime of Eu^{3+} from $Eu(CF_3SO_3)_3$ in a) 0.01 M $HClO_4$ in H_2O ($x_{D/H} = 0$) and b) 0.01 M $DClO_4$ in D_2O ($x_{D/H} = 1$) as a function of concentration. Line is a guide to the eyes only.

Europium(III) photophysics and the Horrocks equation. Figure 4 (and Figures S17-S23) shows the time-resolved emission decay profiles and excited state lifetimes of in the seven water/heavy water mixtures (samples Eu1-Eu7). At each heavy water mole fraction five different concentrations of europium(III) is used. The emission decay profiles can all be fitted using a single exponential decay function. In the pure heavy water sample (Eu7) there is a clear decrease in the

excited state lifetime (Figure 4d) at higher concentrations due to self-quenching effects. For the Eu1-Eu6 (Figures S17-S22) the excited lifetime is, within the experimental uncertainty, constant at all concentrations. As $x_{D/H}$ increases the excited state lifetime increases exponentially (Figure 6b). This is expected as the efficient O-H quenching pathway is removed.[24, 29, 33]

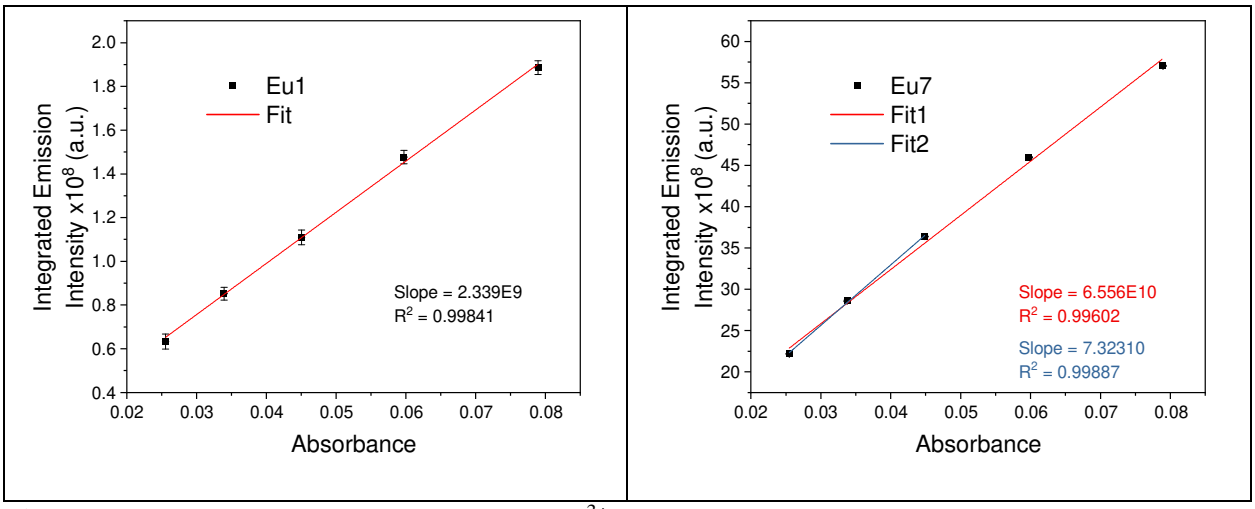

Figure 5. Integrated emission intensity of Eu^{3+} from $Eu(CF_3SO_3)_3$ in left) 0.01 M $HClO_4$ in H_2O ($x_{D/H}$ = 0) and right) 0.01 M $DClO_4$ in D_2O ($x_{D/H}$ = 1) as a function of absorption. For Eu1 the full data set has been fitted with a linear function. For Eu7 the data has been fitted with a linear function for the full data set (Fit1, red) and the 3 lowest concentration points (Fit2, blue).

Figure 5 (and Figures S25-S32) show the emission intensity as a function of absorbance for Eu1-Eu7 as well as for the reference C-153. The emission intensity was taken as the full mathematical area of the corrected (see experimentals) emission spectrum on a wavenumber scale. The absorbance was taken as the absorbance at the excitation wavelength as the slits in the absorption measurement and the excitations slits in the emission measurement were the same (2 nm). The emission intensity as a function of absorbance of C-153 is linear, showing linearity of the detectors (Figure S32). Eu1-Eu4 show good linearity. For Eu5-Eu7 the self-quenching comes into effect. For those 3 samples a fit was made with all the points (red) and one with only the 3 lowest

concentration points (blue). The 3-point fit will be used for quantum yield determinations to lower the influence of the self-quenching effect. Including all the points will change the determined properties less than 2, 3 and 5 relative% for Eu5, Eu6 and Eu7 respectively. From the 35 data points: absorption and emission spectra, and using Coumarin-153 as a reference[30], we can determine the quantum yields for the seven samples.[30-32] Using the luminescence lifetimes we can then calculate the radiative rate constant, non-radiative rate constant, q and $\boldsymbol{A}_{\mathrm{rel}}$.

The photophysical properties of $[Eu(H_2O)_9]^{3+}$ in a TTP coordination geometry are summarized in Table 2 and visualized in Figure 6. The quantum yield increases exponentially as the $x_{D/H}$ increases (Figure 6a). As can be seen from the quantum yield and the excited state lifetime even a small amount of H_2O drastically quenches the emission of europium(III). As expected, the radiative rate is constant across the series, which further support our claim of constant speciation. The non-radiative rate constant decreases linearly as the $x_{D/H}$ is increases (Figure 6c), and is the factor determining the drastic increase in the luminescence quantum yield.

From the k_{nr} we can extrapolate the quenching constant of H_2O k_{OH} for the $[Eu(H_2O)_9]^{3+}$ ion. k_{nr} can be defined a :

$$k_{\mathrm{nr}} = k_{\mathrm{OH}} \cdot x_{\mathrm{H/D}} + k_{\mathrm{outer}} \cdot x_{\mathrm{H/D}} + k_{\mathrm{other}} \qquad \text{eq. 10}$$

Where k_{OH} is the quenching constant of H_2O coordinated at the lanthanide center, $x_{H/D}$ is the mole fraction of H_2O v D_2O, k_{outer} is outer sphere contribution from the solvent, and k_{other} is the rate constant of other non-radiative pathways. By fitting k_{nr} with a linear function (Figure S39) we determine $k_{OH} + k_{outer}$ to be 8388 s^{-1} and k_{other} as 149 s^{-1}. From this, we can conclude that O-H oscillators contributes to 98% of the quenching of emission in the $[Eu(H_2O)_9]^{3+}$ ion. It should be noted that the quenching efficiency of H_2O is highly distance dependent,[24] so the k_{OH} we determine cannot be used universally. q also decreases linearly with $x_{/H}$ (Figure 6d). The q determined here

are higher than those expected as it is well established that the coordination number of europium(III) in water is 9.[25-26, 28, 42] Assuming coordination number 9, we can calculate the expected q, (q') using the mole fraction, $x_{D/H.}$ This is compared to the experimentally determined q in Figure S38. Especially at higher $x_{H/D}$ the q' deviates from the linear trend. This discrepancy has been observed before, however, the cause is not known.[9] Fitting q' with a linear function (Figure S40) gives a slope of 1.07±0.02. While the fit shows a good R^2 value (0.99809) the pure water sample is a clear outlier. Removing this point from the fit gives a near perfect linear fit (R^2 = 0.99998) with a slope of 1.11±0.002. The same deviation from linearity for the pure water sample is seen in the experimentally determined q values (Figure 6d). Both slopes are comparable to the A value of 1.2 used in the Modified Horrocks Equation[24, 33] but are interestingly closer to the value of A = 1.05 used in the Original Horrocks Equation[29].

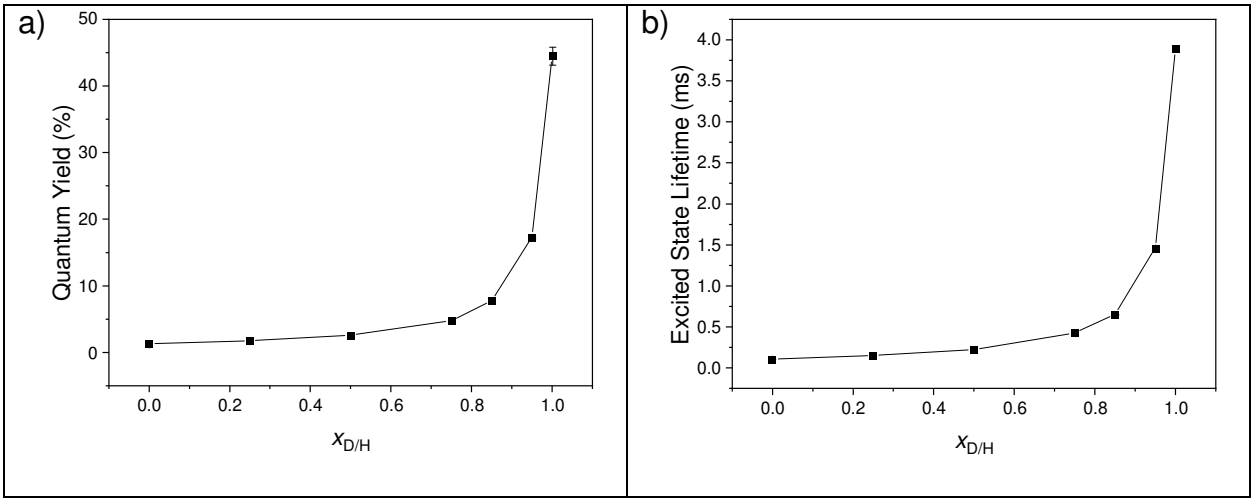

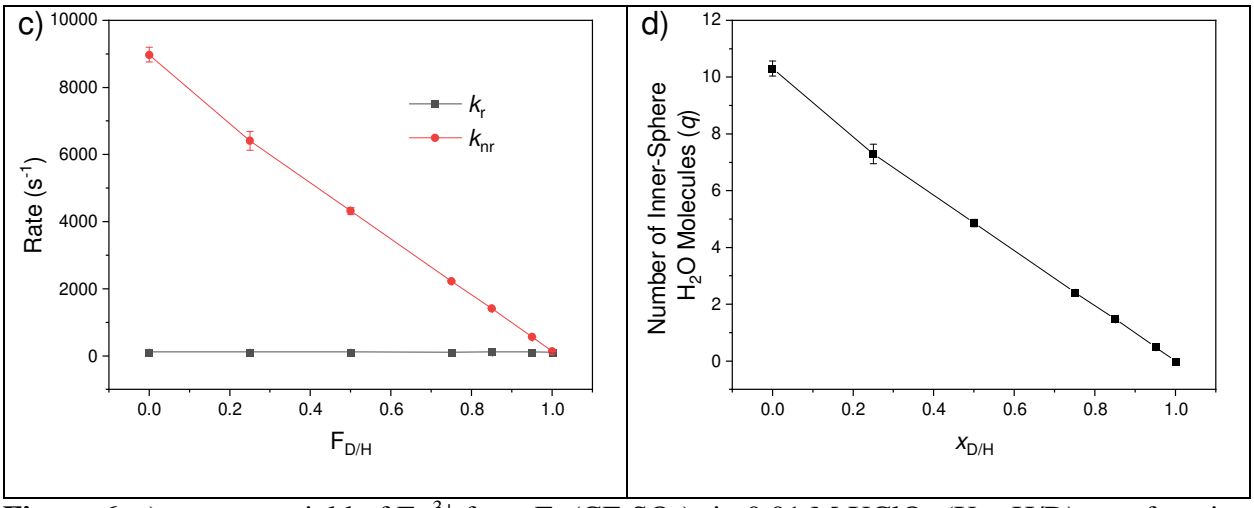

Figure 6. a) quantum yield of Eu^{3+} from $Eu(CF_3SO_3)_3$ in 0.01 M $XClO_4$ (X = H/D) as a function of $x_{D/H}$. b) excited state lifetime of Eu^{3+} from $Eu(CF_3SO_3)_3$ in 0.01 M $XClO_4$ (X = H/D) as a function of $x_{D/H}$. c) radiative and non-radiative rate constants of Eu^{3+} from $Eu(CF_3SO_3)_3$ in 0.01 M $XClO_4$ (X = H/D) as a function of $x_{D/H}$. d) number of inner-sphere H_2O molecules (q) of Eu^{3+} from $Eu(CF_3SO_3)_3$ in 0.01 M $XClO_4$ (X = H/D) as a function of $x_{D/H}$.

Using A_{rel}. Determining $A \equiv k_r$ requires using a dilution series and at least one standard. Determining A_{rel} requires an absorption spectrum, an emission spectrum, and a luminescence lifetime. This is significantly simpler, and we claim the structural information, that changes transition probabilities, are equally well communicated by $A \equiv k_r$ and A_{rel}. This requires that the relative change in the two are the same. As A_{rel} shows the exact same trend as k_r, see Figure 7, we consider this a proven fact. Thus it is shown that A_{rel} is an efficient substitute for k_r for the correct systems. It is important to note that while A_{rel} is corrected for concentration and quenching, the determined value is instrument specific. Therefore, comparisons between samples measured on different instruments or with different settings should only be done with great care. We recommend that binding studies, or studies of europium(III) coordination geometry, are performed using the same instruments and identical settings. If done so, the relative transition probability A_{rel} will

inform exclusively on any changes in the coordination sphere of europium(III). All the effects that may give rise to artifacts or wrong conclusions, when using emission intensity will have been removed.

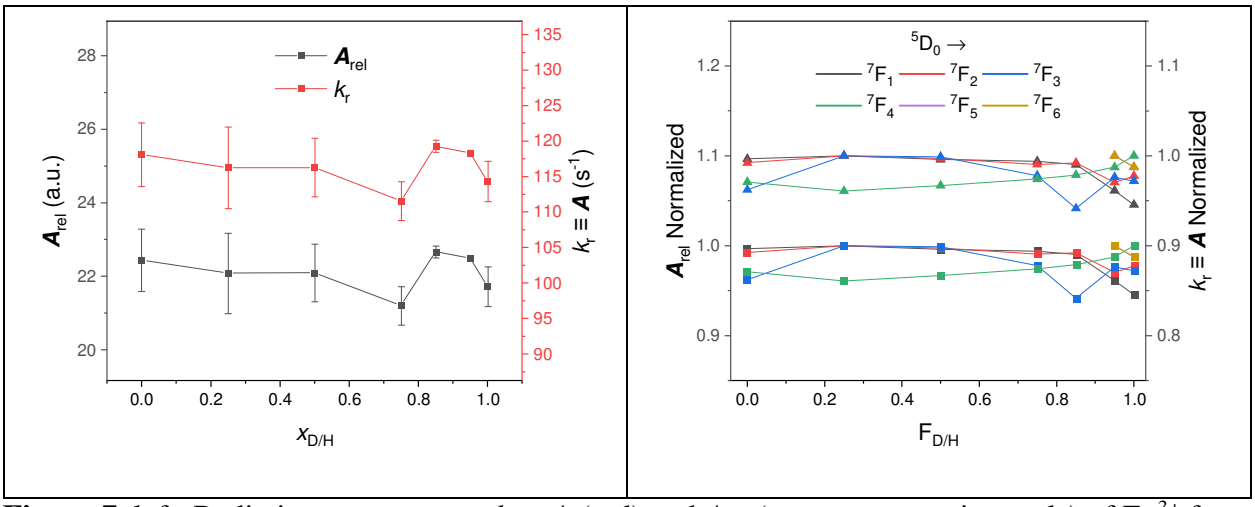

Figure 7. left: Radiative rate constant $k_r \equiv \boldsymbol{A}$ (red) and $\boldsymbol{A}_{rel}$ (grey, see experimentals) of Eu^{3+} from $Eu(CF_3SO_3)_3$ in 0.01 M $XClO_4$ (X = H/D) as a function of $x_{D/H}$. right: normalized branching ratios of emission as $k_r \equiv \boldsymbol{A}$ (triangles) or $\boldsymbol{A}_{rel}$ (squares) of Eu^{3+} from $Eu(CF_3SO_3)_3$ in 0.01 M $XClO_4$ (X = H/D) as a function of $x_{D/H}$

The europium(III) aqua ion. Having established speciation and determined the photophysical properties of europium(III) coordinated to nine water molecules in a tricapped trigonal prismatic coordination geometry, let us consider the results. Across the seven water/heavy water mixtures the the rate of spontaneous emission and radiative lifetime remains constant at 116±2 s^{-1} and 8.6±0.2 ms respectively. The non-radiative deactivation not related to O-H or O-D oscillators was determined to be 143 s^{-1}, which leads to a quantum yield of luminescence of 44 % in heavy water, and 1.3 % in water. In water, the deactivation of the $^5D_0$ level is dominated—unsurprisingly—by deactivation via energy transfer to O-H oscialltors (k_{OH} = 8838 s^{-1} vs. $k_r + k_{nr}$ = 257 s^{-1}) resulting in the low quantum yield.

We can take a step further, and consider the rate of emission from $^5D_0$ to the individual ^7F_J levels, by fractioning quantum yields in the individual bands of the spectrum. This analysis is historically called investigating the branching ratio. The ratio changes with changes in speciation, as each line of the spectrum changes in intensity, *vide infra*. The data for the $[Eu(H_2O)_9]^{3+}$ ion is compiled in Table 3. We have previously treated this subject in detail[23], here we note that also this analysis is done equally well using $k_r \equiv \boldsymbol{A}$ and $\boldsymbol{A}_{rel}$, see figure 7b.

Using the oscillator strength as a descriptor we can first consider the different bands in the europium(III) spectrum. The bands separate in three groups. The high transition probability bands where individual transitions have an oscillator strength (f) of ~2-5$\cdot 10^{-8}$. These are the transitions between $^5D_0$ and $^7F_1$, $^7F_2$, and $^7F_4$. In an asymmetric ligand field, the transition to $^7F_0$, can also be in this group[13, 23], in this case it is vanishing and should be counted as one of the low transition probability bands, which are between $^5D_0$ and $^7F_0$, $^7F_5$, and $^7F_6$ with oscillator strengths below $0.6\cdot 10^{-9}$ for the individual lines. Finally the transitions between $^5D_0$ and $^7F_3$, with f~$0.1\cdot 10^{-8}$, falls in between the two groups.

The oscillator strength and the $\boldsymbol{A}$ values are intechangeable as expetrimental descriptors—and so is the radiative lifetime—and can for organic molecules with allowed transitions be related to electronic structure, Franck-Condon factors and computed spectra. Individual transitions between distinct electronic energy levels have been grouped according to oscillator strength and whether they are forbidden due one or more parameters.[43] First distinguishing between spin allowed ($1<f<10^{-4}$, fluorescence) and spin forbidden ($10^{-4}<f<10^{-9}$ phosphorescence) transitions. Secondly, fluorescence can be symmetry allowed ($1<f<10^{-3}$) or forbidden ($10^{-2}<f<10^{-4}$). The spin forbidden transitions can also be allowed or forbidden, here the distinction is made based on whether the Franck-Condon factor is vanishing ($10^{-6}<f<10^{-9}$) or not ($10^{-7}<f<10^{-9}$). Taking these considerations

into account, the observed oscillator strength in the europium(III) aqua ion ($10^{-8}<f<10^{-10}$) should be expected as all transitions are both spin-forbidden and general angular momentum forbidden and has a vanishing Franck-Condon factor. The Franck-Condon factor is nominally zero due to both symmetry and the intrinsic lack of orbital overlap. Nevertheless, we can group each set of transitions—each band—as less of more forbidden. Having done this analysis we can confirm that the high luminescence quantum yield of europium(III) has nothing to do with particularly allowed transitions,[11] and all to due with the lack of quenching.[24, 29, 33]

Table 2. Photophysical properties of europium(III) in seven water/heavy water mixtures. The symbols have their customary meaning.

Sample	$x_{D/H}$	ϕ_{Lum} (%)	$\boldsymbol{A}_{rel}$[a] (a.u.)	$k_r \equiv \boldsymbol{A}$ (s^{-1})	k_{nr} (s^{-1})	τ_{obs} (μs)	q[b]	q'[c]
Eu1	0	1.3	22.4	118	8971	110	10.3	9
Eu2	0.25	1.8	22.1	116	6411	153	7.3	6.75
Eu3	0.50	2.6	22.1	116	4325	225	4.9	4.5
Eu4	0.75	4.8	21.2	112	2229	427	2.4	2.25
Eu5	0.85	7.8	22.7	119	1412	653	1.5	1.35
Eu6	0.95	17	22.5	118	567	1460	0.5	0.45
Eu7	1	44	21.7	114	143	3886	0	0

[a]see experimentals. [b]from Horrocks Equation[24, 29] (see experimentals). [c]Expected q assuming coordination number 9 (see main text)

Table 3. Photophysical properties of the individual bands of Eu^{3+} from $Eu(CF_3SO_3)_3$ in water/heavy water mixtures. The values are taken as averages of the values obtained from 7 different samples. The values remain constant over the water/heavy water mixtures (see Figure 7).

Transition[a,b]	Branching Ratio[c]	$k_r \equiv \boldsymbol{A}$ (s^{-1}) [c]	f x10^{-7} [c,d]
$^5D_0 \rightarrow {}^7F_1$ (3)	0.39 (0.13)	45 (15)	1.6 (0.52)
$^5D_0 \rightarrow {}^7F_2$ (5)	0.23 (0.046)	27 (5.4)	1.0 (0.2)
$^5D_0 \rightarrow {}^7F_3$ (7)	0.016 (0.0023)	1.9 (0.27)	0.080 (0.011)
$^5D_0 \rightarrow {}^7F_4$ (9)	0.36 (0.040)	42 (4.7)	2.0 (0.22)
$^5D_0 \rightarrow {}^7F_5$ (11)	0.0035 (0.00032)	0.41 (0.037)	0.023 (0.0021)
$^5D_0 \rightarrow {}^7F_6$ (13)	0.009 (0.00071)	1.1 (0.082)	0.073 (0.0056)
Total	1	116	4.8

[a]The $^5D_0 \rightarrow {}^7F_0$ transition is not resolved in the spectra, but is well known to be 0 in the $[Eu(H_2O)_9]^{3+}$ ion (see figure S42). [b]The number in parenthesis denotes the number of m_J microstates within the ^SL_J term. [c]The value in parenthesis denotes the value divided by the m_J degeneracy [d]calculated using Eq. 5.11 from[44]

Conclusions

Here, we present an extensive photophysical characterization of the $[Eu(H_2O)_9]^{3+}$ ion in aqueous solution and put it into a framework consistent with general molecular photophysics.[34-35, 44-45] We conclude that the europium(III) ion is an a tricapped trigonal prismatic (TTP) coordination environment, with a fixed speciation across all samples used here. To our knowledge this is the first photophysical investigation of a single lanthanide(III) ion in solution at this level of detail. The results showed that k_r remains constant across 35 samples in water/heavy water mixtures, and that k_{nr} decreases linearly with mole fraction of heavy water ($x_{D/H}$).

Using seven water/heavy water mixtures we mapped the non-radiative quenching due to O-H oscillators in the solvent. We found that the spectral shape and molar absorptivity remains constant regardless of the $x_{D/H}$, while emission intensity and excited state lifetime increases exponentially

as O-H oscillators are removed. At higher $x_{D/H}$ we once again find evidence of a collisional self-quenching effect.

We elaborated on the $\boldsymbol{A}_{rel}$ treatment, we have introduced previously. We in detail show that $\boldsymbol{A}_{rel}$ gives the exact same trend as the full determination of $k_r \equiv \boldsymbol{A}$. Thus, we conclude that $\boldsymbol{A}_{rel}$ is a valid method to by-pass the laborious quantum yield determinations, and propose that $\boldsymbol{A}_{rel}$ should be used in experiments relying on europium(III) centred interactions to report on a physicochemical property if reliable results are to be extracted from emission spectra.

ASSOCIATED CONTENT

Supporting Information.

Sample composition; all optical spectra: absorption, emission, time-resolved emission decays; and photophysical parameters (PDF). This material is available free of charge via the Internet at http://pubs.acs.org.

AUTHOR INFORMATION

Corresponding Author

Thomas Just Sørensen – Nano-Science Center and Department of Chemistry, University of Copenhagen, 2100, København Ø, Denmark; Orcid: 0000-0003-1491-5116

Nicolaj Kofod – Nano-Science Center and Department of Chemistry, University of Copenhagen, 2100, København Ø, Denmark; Orcid: 0000-0003-2905-8938

Patrick Nawrocki – Nano-Science Center and Department of Chemistry, University of Copenhagen, 2100, København Ø, Denmark; Orcid: 0000-0003-0052-3066

Notes

The authors declare no competing financial interests.

Acknowlegdements. The authors thank Carlsbergfondet, Villum Fonden (grant#14922), the University of Copenhagen, the Danish Chemical Society, and Fulbright Denmark for support.

References

1. Siitari, H.; Hemmilä, I.; Soini, E.; Lövgren, T.; Koistinen, V., Detection of hepatitis B surface antigen using time-resolved fluoroimmunoassay. *Nature* **1983,** *301* (5897), 258-260.
2. Hemmilä, I.; Dakubu, S.; Mukkala, V.-M.; Siitari, H.; Lövgren, T., Europium as a label in time-resolved immunofluorometric assays. *Analytical Biochemistry* **1984,** *137* (2), 335-343.
3. Heffern, M. C.; Matosziuk, L. M.; Meade, T. J., Lanthanide probes for bioresponsive imaging. *Chem Rev* **2014,** *114* (8), 4496-539.
4. Eliseeva, S. V.; Bunzli, J. C., Lanthanide luminescence for functional materials and bio-sciences. *Chemical Society reviews* **2010,** *39* (1), 189-227.
5. Dragic, P. D.; Cavillon, M.; Ballato, J., Materials for optical fiber lasers: A review. *Applied Physics Reviews* **2018,** *5* (4), 041301.
6. Heller, A., Liquid lasers—Fluorescence, absorption and energy transfer of rare earth lon solutions in selenium oxychloride. *Journal of Molecular Spectroscopy* **1968,** (28), 208–232.
7. Hilborn, R. C., Einstein coefficients, cross sections, f values, dipole moments, and all that. *American Journal of Physics* **1982,** *50* (11), 982-986.
8. Kasha, M., 50 YEARS OF THE JABLONSKI DIAGRAM. *Acta Phys. Pol. A* **1987,** *71* (5), 661-670.
9. Nawrocki, P. R.; Kofod, N.; Juelsholt, M.; Jensen, K. M. Ø.; Sørensen, T. J., The effect of weighted averages when determining the speciation and structure–property relationships of europium(iii) dipicolinate complexes. *Physical Chemistry Chemical Physics* **2020,** *22* (22), 12794-12805.
10. Nielsen, L. G.; Sørensen, T. J., Including and Declaring Structural Fluctuations in the Study of Lanthanide(III) Coordination Chemistry in Solution. *Inorganic Chemistry* **2019,** *59* (1), 94-105.
11. Kofod, N.; Arppe-Tabbara, R.; Sørensen, T. J., Electronic Energy Levels of Dysprosium(III) ions in Solution. Assigning the Emitting State and the Intraconfigurational 4f–4f Transitions in the Vis–NIR Region and Photophysical Characterization of Dy(III) in Water, Methanol, and Dimethyl Sulfoxide. *The Journal of Physical Chemistry A* **2019,** *123* (13), 2734-2744.
12. Kofod, N.; Nawrocki, P.; Platas-Iglesias, C.; Sørensen, T. J., Electronic Structure of Ytterbium(III) Solvates—a Combined Spectroscopic and Theoretical Study. *Inorganic Chemistry* **2021,** *60* (10), 7453-7464.
13. Kofod, N.; Nawrocki, P.; Juelsholt, M.; Christiansen, T. L.; Jensen, K. M. Ø.; Sørensen, T. J., Solution Structure, Electronic Energy Levels, and Photophysical Properties of $[Eu(MeOH)_{n-2m}(NO3)_m]^{3-m+}$ Complexes. *Inorganic Chemistry* **2020**.
14. Web of Science. (accessed 09/12-2021).

15. Junker, A. K. R.; Tropiano, M.; Faulkner, S.; Sørensen, T. J., Kinetically inert lanthanide complexes as reporter groups for binding of potassium by 18-crown-6. *J Inorganic chemistry* **2016,** *55* (23), 12299-12308.
16. Bridou, L.; Nielsen, L. G.; Sørensen, T. J., Using europium(III) complex of 1,4,7,10-tetraazacyclododecane-1,4,7-triacedic acid Eu.DO3A as a luminescent sensor for bicarbonate. *Journal of Rare Earths* **2020,** *38* (5), 498-505.
17. Bünzli, J.-C. G.; Piguet, C., Taking advantage of luminescent lanthanide ions. *Chemical Society Reviews* **2005,** *34* (12), 1048-1077.
18. Allain, C.; Beer, P. D.; Faulkner, S.; Jones, M. W.; Kenwright, A. M.; Kilah, N. L.; Knighton, R. C.; Sørensen, T. J.; Tropiano, M., Lanthanide appended rotaxanes respond to changing chloride concentration. *Chemical Science* **2013,** *4* (1), 489-493.
19. Tropiano, M.; Blackburn, O. A.; Tilney, J. A.; Hill, L. R.; Placidi, M. P.; Aarons, R. J.; Sykes, D.; Jones, M. W.; Kenwright, A. M.; Snaith, J. S.; Sørensen, T. J.; Faulkner, S., Using Remote Substituents to Control Solution Structure and Anion Binding in Lanthanide Complexes. **2013,** *19* (49), 16566-16571.
20. Vereb, G.; Jares-Erijman, E.; Selvin, P. R.; Jovin, T. M., Temporally and Spectrally Resolved Imaging Microscopy of Lanthanide Chelates. *Biophysical Journal* **1998,** *74* (5), 2210-2222.
21. Walton, J. W.; Bourdolle, A.; Butler, S. J.; Soulie, M.; Delbianco, M.; McMahon, B. K.; Pal, R.; Puschmann, H.; Zwier, J. M.; Lamarque, L., Very bright europium complexes that stain cellular mitochondria. *Chemical Communications* **2013,** *49* (16), 1600-1602.
22. Picot, A.; D'Aléo, A.; Baldeck, P. L.; Grichine, A.; Duperray, A.; Andraud, C.; Maury, O., Long-Lived Two-Photon Excited Luminescence of Water-Soluble Europium Complex: Applications in Biological Imaging Using Two-Photon Scanning Microscopy. *Journal of the American Chemical Society* **2008,** *130* (5), 1532-1533.
23. Kofod, N.; Nielsen, L. G.; Sørensen, T. J., Temperature Dependence of Fundamental Photophysical Properties of $[Eu(MeOH\text{-}d_4)_9]^{3+}$ Solvates and $[Eu{\cdot}DOTA(MeOH\text{-}d_4)]^-$ Complexes. *The Journal of Physical Chemistry A* **2021,** *125* (38), 8347-8357.
24. Beeby, A.; M. Clarkson, I.; S. Dickins, R.; Faulkner, S.; Parker, D.; Royle, L.; S. de Sousa, A.; A. Gareth Williams, J.; Woods, M., Non-radiative deactivation of the excited states of europium, terbium and ytterbium complexes by proximate energy-matched OH, NH and CH oscillators: an improved luminescence method for establishing solution hydration states. *Journal of the Chemical Society, Perkin Transactions 2* **1999,** (3), 493-504.
25. Binnemans, K., Interpretation of europium(III) spectra. *Coordination Chemistry Reviews* **2015,** *295*, 1-45.
26. Binnemans, K.; Van Herck, K.; Görller-Walrand, C., Influence of dipicolinate ligands on the spectroscopic properties of europium(III) in solution. *Chemical Physics Letters* **1997,** *266* (3), 297-302.
27. Flanagan, B. M.; Bernhardt, P. V.; Krausz, E. R.; Lüthi, S. R.; Riley, M. J., A Ligand-Field Analysis of the trensal (H3trensal= 2, 2 ‘, 2 ‘‘-Tris (salicylideneimino) triethylamine) Ligand. An Application of the Angular Overlap Model to Lanthanides. *Inorganic chemistry* **2002,** *41* (20), 5024-5033.
28. Parker, D.; Dickins, R. S.; Puschmann, H.; Crossland, C.; Howard, J. A., Being excited by lanthanide coordination complexes: aqua species, chirality, excited-state chemistry, and exchange dynamics. *Chem Rev* **2002,** *102* (6), 1977-2010.

29. Horrocks Jr, W. D.; Sudnick, D. R., Lanthanide ion probes of structure in biology. Laser-induced luminescence decay constants provide a direct measure of the number of metal-coordinated water molecules. *Journal of the American Chemical Society* **1979,** *101* (2), 334-340.
30. Würth, C.; Grabolle, M.; Pauli, J.; Spieles, M.; Resch-Genger, U., Relative and absolute determination of fluorescence quantum yields of transparent samples. *Nature Protocols* **2013,** *8* (8), 1535-1550.
31. Brouwer, A. M., Standards for photoluminescence quantum yield measurements in solution (IUPAC Technical Report). *Pure and Applied Chemistry* **2011,** *83* (12), 2213-2228.
32. Resch-Genger, U.; Hoffmann, K.; Nietfeld, W.; Engel, A.; Neukammer, J. a.; Nitschke, R.; Ebert, B.; Macdonald, R., How to improve quality assurance in fluorometry: fluorescence-inherent sources of error and suited fluorescence standards. *Journal of Fluorescence* **2005,** *15* (3), 337-362.
33. Tropiano, M.; Blackburn, O. A.; Tilney, J. A.; Hill, L. R.; Sørensen, T. J.; Faulkner, S., Exploring the effect of remote substituents and solution structure on the luminescence of three lanthanide complexes. *Journal of Luminescence* **2015,** *167*, 296-304.
34. Strickler, S.; Berg, R. A., Relationship between absorption intensity and fluorescence lifetime of molecules. *The Journal of chemical physics* **1962,** *37* (4), 814-822.
35. Hirayama, S.; Phillips, D., Correction for refractive index in the comparison of radiative lifetimes in vapour and solution phases. *Journal of Photochemistry* **1980,** *12* (2), 139-145.
36. de Bettencourt-Dias, A., *Luminescence of lanthanide ions in coordination compounds and nanomaterials*. John Wiley & Sons: 2014.
37. Tanner, P. A., Some misconceptions concerning the electronic spectra of tri-positive europium and cerium. *Chemical Society Reviews* **2013,** *42* (12), 5090-5101.
38. Thomsen, M. S.; Madsen, A. Ø.; Sørensen, T. J., Crystal structure and optical properties of a two-sited EuIII compound: an EuIII ion coordinated by two [EuIII (DOTA)]− complexes (DOTA is 1, 4, 7, 10-tetraazacyclododecane-1, 4, 7, 10-tetraacetate). *Acta Crystallographica Section C: Structural Chemistry* **2021,** *77* (7).
39. Parker, D.; Suturina, E. A.; Kuprov, I.; Chilton, N. F. J. A. o. C. R., How the ligand field in lanthanide coordination complexes determines magnetic susceptibility anisotropy, paramagnetic NMR shift, and relaxation behavior. **2020,** *53* (8), 1520-1534.
40. Parker, D.; Fradgley, J.; Zwier, J. M.; Walton, J. W.; Delbianco, M.; starck, m., Comparative analysis of lanthanide excited state quenching by electronic energy and electron transfer processes. *Faraday Discussions* **2021**.
41. Carnall, W. T.; Fields, P. R.; Rajnak, K., Electronic Energy Levels of the Trivalent Lanthanide Aquo Ions. IV. Eu3+. **1968,** *49* (10), 4450-4455.
42. Marmodée, B.; Jahn, K.; Ariese, F.; Gooijer, C.; Kumke, M. U., Direct Spectroscopic Evidence of 8- and 9-fold Coordinated Europium(III) Species in H2O and D2O. *The Journal of Physical Chemistry A* **2010,** *114* (50), 13050-13054.
43. Kasha, M., From Jablonski to femtoseconds. Evolution of molecular photophysics. *Acta Phys. Pol. A* **1999**, 15-36.
44. Turro, N. J., *Modern Molecular Photophysics*. University Science Books: Sausalito, California, 1978.
45. Valaur, B.; Berberan-Santos, M. N., *Molecular Fluorescence*. 2nd ed.; Wiley-VCH: 2012.